Journal of Inflammation Research

Dovepress
Taylor & Francis Group

Open Access Full Text Article

ORIGINAL RESEARCH

Thymosin β4 Regulates Tissue Inflammatory Response in Mouse Nonalcoholic Fatty Liver Disease by Promoting Macrophage M2-Type Polarization

Zixin Zhu[1,*], Yifan Liao[2,*], Qiuju Mou[1], Hongjie Liu[2], Yuxue Shen[2], Lili Zhu[1], Shuo Cong[1]

[1]Department of Blood Transfusion, The Affiliated Hospital of Guizhou Medical University, Guiyang, 550004, People's Republic of China; [2]School of Clinical Laboratory Science, Guizhou Medical University, Guiyang, 550004, People's Republic of China

*These authors contributed equally to this work

Correspondence: Shuo Cong, Email 2022120040826@stu.gmc.edu.cn

Introduction: Nonalcoholic fatty liver disease (NAFLD) is characterized by hepatic steatosis, insulin resistance, and systemic pro-inflammatory response. Thymosin β4 (Tβ4) is a bioactive polypeptide that inhibits extracellular matrix (ECM) deposition and protects the liver. It can achieve immune homeostasis by regulating the polarization of liver macrophages and is a potential treatment for NAFLD.

Methods: A dataset was used to evaluate the expression of Tβ4 in fatty and non-fatty adjacent tissues of primary hepatocellular carcinoma. NAFLD was induced in C57 mice with methionine and choline-deficient diet (MCD), siRNATβ4 was injected into the tail vein to reduce liver Tβ4, and the therapeutic effect of Tβ4 was observed by phagocytosis of macrophages with clodronate liposomes. Hematoxylin and Eosin staining (HE) staining was used to observe the inflammation of mice in each group, and oil red O staining was used to determine the lipid accumulation. Macrophage polarization was detected by immunofluorescence assay. In the extrachromosomal experiment of oil red O, human myeloid leukemia mononuclear (THP-1) cells was co-cultured with human hepatic (LO2) constructed with oleic acid to detect the changes of aspartate transaminase (AST) and alanine transaminase (ALT) in supernatant and the apoptosis of LO2 under the intervention of different concentrations of Tβ4.

Results: Tβ4 allowed the mice to recover from NAFLD and reduce liver inflammation more effectively. Liver steatosis was more severe in sirnat4 mice. Macrophages are involved in Tβ4 treatment of NAFLD. The expression level of M1 phenotype in macrophages treated with Tβ4 decreased, and the apoptosis of hepatocytes decreased. At the same time, Tβ4 down-regulates signal transduction and activator of transcription1 (STAT1) phosphorylation and increases suppressor of cytokine signaling1/3 (SOCS1/3) expression in hepatocytes.

Discussion: This study revealed the molecular mechanism of the effective effect of Tβ4 on the polarization of liver macrophages, suggesting that Tβ4 may be a potential therapeutic measure for NAFLD.

Keywords: thymosin beta 4, NAFLD, macrophage, inflammation

Introduction

NAFLD consists of a continuum of liver disease with early symptoms of simple hepatic steatosis. As repeated inflammatory infiltration is accompanied by hepatocellular damage,[1] NAFLD can progress to non-alcoholic steatohepatitis (NASH) and eventually to irreversible cirrhosis and hepatocellular carcinoma (HCC), with an exponential increase in mortality as the disease progresses. Although the histopathological features of NAFLD are similar to those of alcohol-related liver disease, the pathogenesis is not the same.[2] NAFLD is considered to be the hepatic manifestation of a metabolic syndrome, often associated with obesity, insulin resistance, hypertension and dyslipidemia.[2] The "multiple

Received: 14 September 2024
Accepted: 15 December 2024
Published: 29 April 2025

parallel hits" hypothesis describes the pathogenesis of NAFLD from simple hepatic steatosis to steatohepatitis. NAFLD affects 10–24% of the global population and is the most common form of chronic liver disease. It is the most common cause of chronic liver disease.[3]

As research into NAFLD progresses, it has become clear that dysregulation of the immune response is an important factor in the development of NAFLD,[4] and that NAFLD patients' hepatic resident cells (Kupffer cells, hepatic stellate cells, etc) and infiltrating immune cells (neutrophils, dendritic cells and macrophages, etc) are influenced by their environment to release pro-inflammatory factors including IL.1, IL.6 and TNF-α, etc, which contribute to the development of NAFLD. As a result of altered intestinal permeability, inflammatory ligands in the circulation increase and are bound by pattern recognition receptors on haematopoietic and non-haematopoietic cells to activate multiple pro-inflammatory cascades that together exacerbate liver injury.[5] Macrophages are the most abundant immune cells in the liver and are important for the development of NAFLD. Macrophages can differentiate into different or even opposite expressions in response to different environmental stimuli and can be simply divided into a pro-inflammatory Ml phenotype polarisation and an anti-inflammatory M2 phenotype polarisation. M1 type macrophages exacerbate disease progression. In a mouse model of NASH, pharmacological induction of macrophage M2-type polarisation reversed steatosis and hepatocyte apoptosis in the liver of mice. M2-type macrophages with anti-inflammatory and repair functions attenuated liver damage and insulin resistance caused by NAFLD.[6] A large body of clinical data and animal disease models suggest that macrophages play an important role in the development of NAFLD. The more severe the disease in NAFLD patients, the higher the number of CD68+ Kupffer cells in their liver biopsies, and the presence of large numbers of activated macrophages between damaged hepatocytes has been found in paediatric NAFLD patients.[7] Removal of macrophages from mouse liver with chlorophosphate liposomes significantly alleviated HFD diet-induced hepatic steatosis and attenuated the hepatic inflammatory response and liver injury. Macrophages promote hepatic steatosis by producing IL1-β to inhibit peroxisome proliferator-activated receptor (PPARα),[8] and PPARa promotes fatty acid oxidation in hepatocytes to prevent hepatic steatosis.[9]

Thymosin beta 4 (Tβ4), an amino acid peptide widely distributed in mammals and other vertebrates, is a natural protein found in a variety of nucleated cells and binds specifically to G-actin to regulate the polymerisation of actin, thereby promoting vascular regeneration, wound healing and hair follicle regeneration.[10] Belsky's study showed that overexpression of Tβ4 in mice reduced the risk of sepsis caused by Legionella in the lung, possibly by a significant reduction in interleukin 1β (IL-1β) and tumour necrosis factor alpha (TNF-α) secretion by lung macrophages.[11] Our previous article has shown that Tβ4 reduces lipid accumulation and oxidative stress during NAFLD by attenuating the iron death effect in hepatocytes. However, the mechanism of whether Tβ4 inhibits NAFLD by regulating macrophage polarization is unclear.[12] Therefore, in this study, the ameliorative effects of Tβ4 on the MCD-induced model and the regulatory pathway on Kupffer cells (KCs) polarization were assessed.

The results suggest that Tβ4 can exert its anti-inflammatory effects by modulating hepatic macrophage polarization, so we further investigated the cell-specific mechanisms of Tβ4-induced macrophage polarization using an LPS-induced inflammation model in a THP-1 cell line. These data provide insightful protocols for enhancing the local immunomodulation and anti-inflammation of NAFLD by Tβ4.

Materials and Methods

Material

SPF grade C57BL/6 male mice, purchased from Changsha Tianqin Laboratory Animal Centre and housed at Guizhou Medical University Laboratory Animal Centre. Tβ4 (98%+ purity) Solebro Biotechnology Ltd; Chloral hydrate Regen Bio Ltd; methanol, ethanol Tianjin Fuyu Chemical Company Ltd; High glycemic DMEM cell culture medium (containing 1% non-essential amino acids, 1% L-glutamine, 1% double antibodies and 10% fetal bovine serum) GIBCO; Apoptosis assay kit KGI Biotechnology Ltd; RNA extraction kit OMEGA Biotechnology; real-time fluorescence quantitative polymerase chain reaction (qPCR) kit Shanghai Biotechnology Co. Ltd.; BCA quantification kit Shanghai Biotec Co. LDL-C, high-density lipoprotein cholesterol (HDL-C), ROS, alanine aminotransferase (ALT), aspartate

aminotransferase (AST), glutathione (GSH) and triglyceride (TG) kits Nanjing Jiancheng Biological Engineering. All other chemicals are of analytical grade.

Animal Breeding

All mice were acclimatised to environmental conditions in communal plastic cages one week before the start of the experiment, housed in SPF animal rooms with room temperature of 20–22°C, humidity of (50±2)%, 12h/12h light/dark cycle, housed in separate cages, fed ad libitum and given their assigned chow. All animal experimental procedures were approved by the Animal Ethics Committee of Guizhou Provincial People's Hospital, which followed the National Institute of Health guidelines for the care and use of laboratory animals. All the mice were randomly divided into four groups of numbers. Normal control group (WT group) was given normal diet without drug treatment. The model group (MCD group) was given the MCD diet without medication. Tβ4 group was given conventional diet, and Tβ4 was intraperitoneally injected 12 mg/kg per day from the 9th week to the end of the 4th week. After receiving the MCD diet for the first eight weeks, the MCD+Tβ4 group was injected with Tβ4 (12 mg/kg) starting at week 9 and ending at week 12.

Cell Cultures

Construction of a Model of Palmitic Acid (PA)-Induced Human Normal Hepatic LO2 Cells

LO2 cells were derived from the cell bank of Shanghai Institute of Biological Sciences, Chinese Academy of Sciences, and STR typing was performed to deny HELA contamination. LO2 cells were grown in DMEM high sugar medium containing 10% fetal bovine serum. After cell differentiation and maturation, LO2 cells were treated with 100 μm PA (purity ≥99.0%, Kuntronics) to construct an in vitro fatty liver model, referring to the experimental method in the article Qi et al, 2012. Cells were cultured at 37.5°C in a humidified incubator containing 5% CO2. Different doses of Tβ4 (1, 5, 10, 20, 40, 80, 100μg/mL) were added to LO2 cells for 24h, and cell viability was measured by CCK8 method. We found that appropriate doses of Tβ4 (≤1390ng/mL) had no significant effect on cell viability. Therefore, we chose a concentration of 1000ng/mL as the experimental dose for the next examination.

Cell Co-Cultivation System

To provide more clarity on the regulation of hepatocytes after Tβ4 affects macrophages. We used a co-culture method of THP-1 and LO2 cells. Establishment of the co-culture model: THP-1 and LO2 cells were cultured in high-sugar DMEM medium containing 10% fetal bovine serum (FBS), 100 U/mL penicillin and 100 μg/mL streptomycin. Cells were placed in a 37°C, 5% CO2 concentration incubator and grown to 80–90% fusion for the next step. THP-1 cells were digested with 0.25% trypsin and passaged, and LO2 were diluted and passaged after blowing down with pre-chilled culture solution at 4°C. Both logarithmic growth phase cells were taken for experiments. THP-1 macrophages were inoculated into 24-well plates at 2×10^5 cells per well, and after the cells had grown to 48h of contact inhibition, the cells were induced to differentiate by the classical "cocktail method" for 10d, and after the mature cells reached 90% or more, the co-culture group placed Transwell chambers inside the 24-well plates to form upper and lower chambers. The upper chamber was interconnected by a 0.45μm polycarbonate membrane, and LO2 human hepatocytes were laid out in 2×10^5 cells per well. The experiment was divided into co-culture control group (model group) and co-culture + Tβ4 treatment group with Tβ4 concentrations of 10ng/mL, 100ng/mL and 1000ng/mL respectively.

Assessment of Biochemical and Lipid Markers

Serum concentrations of alanine aminotransferase (ALT), aspartate aminotransferase (AST) and each of the total cholesterol (TC), triglycerides (TG), low-density lipoprotein cholesterol (LDL-C), high-density lipoprotein cholesterol (HDL-C), indicators Interleukin2/6(IL-2, IL-6) and d tumor necrosis factor-α (TNF-α) were measured using the assay kit.

Oxidative Stress Parameters Testing

The concentrations of superoxide dismutase (SOD), malondialdehyde (MDA, No. A003-1-2), and glutathione peroxidase (GSH-Px, No. A005-1-2) were assessed using commercial kits purchased from Nanjing Jiancheng Bioengineering (Jiangsu) Co., China) according to the manufacturer's instructions.

Reactive Oxygen Species (ROS) Testing

Assessment of ROS concentrations in trypsin-digested single cell suspensions of liver tissue using DCFH-DA-ROS from Nanjing Jiancheng Institute of Biological Engineering.

Pathological Histology Observation

After execution of the rats, liver tissue was immersed in 10% formalin buffer (pH=7.4) for 24 hours, embedded in paraffin, then thick sections (4 μm, Microm GmbH, Germany) were cut and stained with hematoxylin and eosin (handE) for lipid droplet assessment. Oil red "O" staining was used to observe the accumulation of lipid droplets in the liver. Immunohistochemistry was performed to F4/80 protein expression levels in rat liver. Paraffin sections were dewaxed to water, washed 3 times with PBS for 3 min/time; antigen repair was performed by heating with sodium citrate repair solution, washed 3 times with PBS for 3 min/time; endogenous peroxidase was removed by adding 30% hydrogen peroxide dropwise for 10 min, washed 3 times with PBS for 3 min/time; normal non-immune animal serum was added dropwise and incubated for 10 min at room temperature for blocking; F4/80 was incubated for 60 min at room temperature. incubate for 60 min at room temperature, discard primary antibody, wash 3 times with PBS, 3 min/time; add biotin-labelled secondary antibody dropwise, incubate for 10 min at room temperature, wash 3 times with PBS, 3 min/time; add Streptomyces anti-biotin protein-peroxidase reagent dropwise, incubate for 10 min at room temperature, wash 3 times with PBS, 3 min/time; add freshly prepared DAB colour development reagent dropwise; wash with PBS, 3 min/time; incubate for 10 min at room temperature, wash with PBS, 3 min/time; incubate for 10 min at room temperature, wash with PBS, 3 min/time. The colour development was terminated by PBS rinsing, hematoxylin re-staining, 1% ethanol hydrochloric acid fractionation, tap water rinsing to return to blue, dehydration and transparency, then neutral gum sealing and observation under light microscope.

Apoptotic Cell Death Assay

Each group was treated with 100 μL of Annexin V FITC conjugate and 5 μL of PI Solution, vortexed and mixed, and incubated for 20 min at room temperature, then incubated on a flow cytometer to detect apoptosis in each group.

Immunofluorescence Localisation Assay

Animal liver tissues were fixed in 4% paraformaldehyde, dehydrated and paraffin embedded, 5 μm thick paraffin sections were prepared; dewaxed to water, antigen repaired by sodium citrate at high pressure, histochemical pen was drawn around the tissue, autofluorescence quencher was added to the circle and bovine serum albumin was closed for 30 min in which immunofluorescence double label staining was performed, primary antibody rabbit anti-pSTAT1 (1:200) was added dropwise, in a wet box The tissue was washed 3 times with PBS and covered with a drop of Cy3-labelled goat anti-rabbit IgG (1:300) of the appropriate species for the primary antibody; incubated for 50 min at room temperature, protected from light; washed 3 times with PBS and incubated for 10 min at room temperature, protected from light, before sealing with an anti-fluorescence quenching sealer.

Realtime RT-PCR Assay

Total RNA was extracted from liver tissues according to the instructions of RNA extraction kit, and the purity and concentration of RNA were determined by Nanodrop Micro Nucleic Acid Assay Instrument, the extracted total RNA was reverse transcribed into cDNA, and the synthesised cDNA was amplified by real-time fluorescence quantitative PCR instrument. Mouse The primer sequences of fluorescence quantitative PCR were synthesised by Bioengineering (Shanghai) Co., Ltd, and the sequences of each primer are shown in Table 1. The relative quantification of mRNA of each gene was carried out by using GAPDH as the internal reference, and the mRNA expression level of each index in liver tissues was calculated by using the 2-ΔΔCT method.

Table 1 Animal Primer Sequences

GENE		Primer
STAT1	F	5'-:CAGAACCGATGGAGGCTTGA-3'
	R	5'-GCAGGTTGTCTGTGGGTCTGA-3'
SOCS1	F	5'-ACACTCACTTCCGCACCTTC-3'
	R	5'-GAAGCCATCTTCACGCTGAG-3'
SOCS3	F	5'-ACCAGCGCCACTTCTTCACG-3'
	R	5'-GTGGAGCATCATACTGATCC-3'
GAPDH	F	5'-AATTCAACGGCACAGTCAA-3'
	R	5'-TGTACTGGGGTCTCGGTCC-3'

Western-Blotting Analysis of Protein Expression Levels

Tissues were lysed by adding appropriate amount of RIPA lysis solution on ice, and the supernatant of total protein was extracted, and the protein concentration was determined by BCA protein concentration kit. An equal amount of protein was taken from each group, 10%SDSPAGE electrophoresis was performed, electro transferred to PVDF membrane, and 5% skimmed milk was closed at room temperature for 1 h. The tissue was incubated overnight in a refrigerator at 4°C with primary mouse anti-pSTAT1, STAT, SOCS1 and SOCS3 (1:1000), rabbit anti-GAPDH polyclonal antibody (1:1000), and incubated in a refrigerator at 4°C with TBT. After incubation in the refrigerator at 4 °C overnight, TBST was rinsed and incubated with the corresponding secondary horseradish peroxidase-labelled goat anti-rabbit IgG (1:2500) or goat anti-mouse at room temperature for 1 h. After rinsing with TBST, the film was exposed by the ECL luminescence method according to the instructions in the kit, and the protein bands were visualized by the chemiluminescence imaging system and the images were collected and analysed by the Flu- orChemHD2 software. orChemHD2 software was used to analyse the grey value of the bands, and the protein concentration was expressed as a percentage of the grey value of the reference band.

Statistical Analysis

Data statistics were performed using SPSS 23.0. All data are the mean ± standard error of mean (mean ± SEM) of three independent experiments. One-way analysis of variance (ANOVA) and post hoc multiple comparison tests were used to compare significant differences between groups. $p<0.05$ was considered statistically significant and $p<0.01$ was considered extremely significant.

Results

Tβ4 Levels Showed Negative Correlation with NAFLD Expression

Expression profiling data of the 2 platforms of GPL13534 and GPL570 were obtained from the GSE dataset, data correction was performed on the 2 expression profiling data and log values were taken, and box line plots were applied to visualise the levels of the Tβ4 gene in NAFLD in NAFLD in the disease process of NAFLD. Tβ4 expression levels were significantly and statistically lower in the disease severity group compared with the disease process severity group (Figure 1A).

To further validate the accuracy of the bioinformatics results, we validated the NAFLD sera collected from the outpatient clinic of the Affiliated Hospital of Guizhou Medical University, as shown in Figure 1B. The serum Tβ4 content of NAFLD patients was significantly lower compared with that of healthy controls. In addition Tβ4 immunofluorescence staining was confirmed in 5 cases of steatotic hepatocellular carcinoma paracellular tissues of hepatocellular carcinoma patients and 5 cases of non-steatotic hepatocellular carcinoma paracellular tissues of patients with hepatocellular carcinoma sourced from the Affiliated Hospital of Guizhou Medical University and the statistical analysis of the StralaQuest software confirmed that the expression of Tβ4 in human steatotic liver tissues was significantly lower than that in non-steatotic liver tissues (Figure 1C).

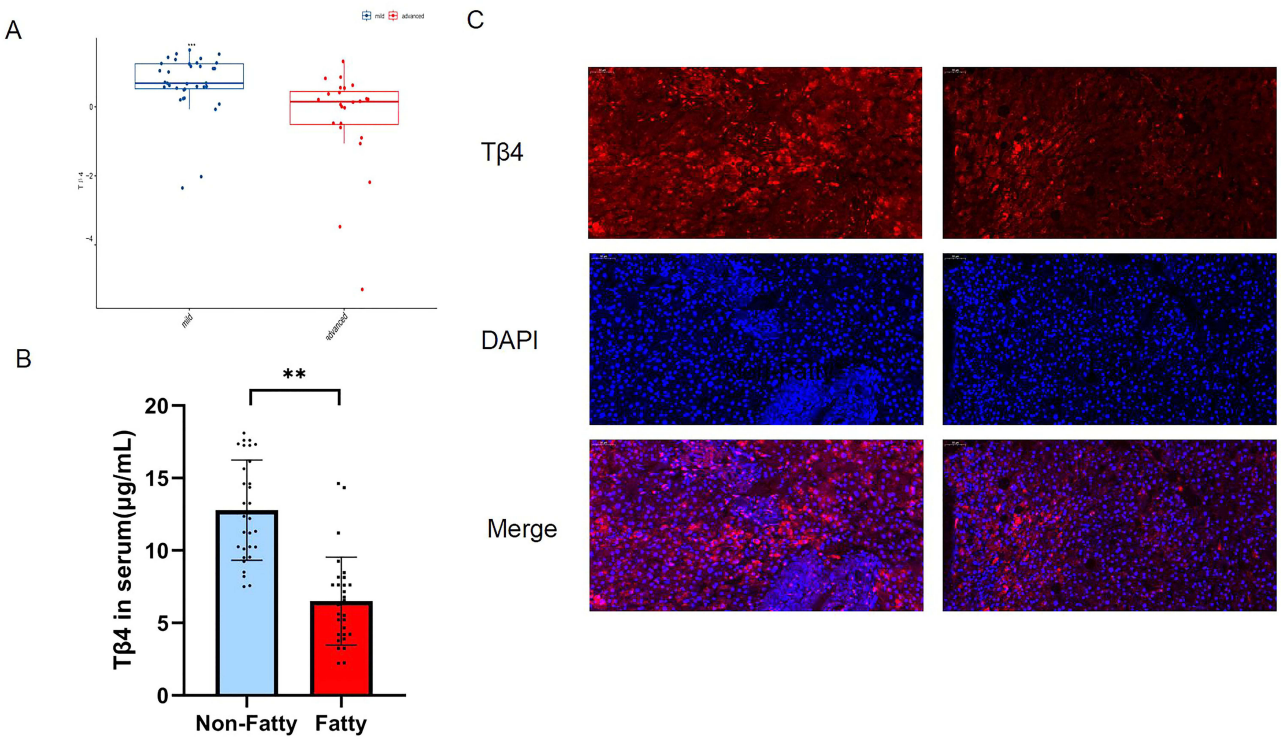

Figure 1 Changes in the level of Tβ4 in NALFD. (**A**) Tβ4 expression is reduced in NALFD disease. (**B**) Low level of Tβ4 expression in serum of NALFD patients. (**C**) Reduced levels of Tβ4 expression in tissues adjacent to steatotic primary hepatocellular carcinoma. **P<0.01.

Tβ4 Attenuates MCD-Induced Hepatic Steatosis and Inflammatory Response

Figure 2A is an effective therapeutic peptide formula for Tβ4. The treatment of mice in the MCD+Tβ4 group was shown in Figure 2B. Compared with mice in the WT group, mice in the MCD group significantly lost weight after Tβ4 injection (Figure 2C), while mice in the MCD group gained liver weight (Figure 2D). After Tβ4 drug treatment, AST and ALT levels decreased (Figure 2E-F) and TP levels increased (Figure 2G). In the livers of Tβ4-treated McD-fed mice, liver sections stained with HE or oil red O (Figure 2H) showed a significant reduction in lipid accumulation and content in the liver.

Tβ4 Inhibits Hepatic Cell Necrosis and Attenuates Oxidative Stress in NAFLD Model Mice

Compared with the normal group, the serum and liver GSH-Px levels of mice in the model group were significantly reduced, and the MDA level was significantly increased; compared with the model group, the serum and liver GSH levels of mice were increased and the MDA level was reduced after Tβ4 treatment (Figure 3A–D); compared with the normal group, the TUNEL-stained liver cell necrosis of mice in the model group was significantly increased, and the fluorescence intensity was reduced by the Tβ4 treatment (Figure 3E), and electron microscopy results showed that the livers of mice in the model group showed more organelle destruction lysis, and the organelle destruction was reduced by Tβ4 treatment (Figure 3F). Compared with the control group, ROS accumulation was significantly higher in the model group; compared with the model group, the fluorescence intensity FITC fluorescence value was the weakest after Tβ4 treatment. The results suggested that Tβ4 effectively inhibited the abnormal accumulation of intracellular reactive oxygen species (Figure 3G).

Tβ4 is Involved in Macrophage Polarisation

Immunohistochemistry results showed that the hepatic F4/80 of mice in the model group was significantly varied, and the hepatic F4/80 expression level of mice was significantly reduced after Tβ4 treatment compared with the model group (Figure 4A). The antibody F4/80 was used to label macrophages, CD206 to label M2 type macrophages. Immunofluorescence double staining of marker CD206, and liver tissues showed that CD206 positive cells were significantly increased and overexpressed in the portal region of liver tissues in both model groups, while CD206 fluorescence intensity was significantly reduced after treatment with

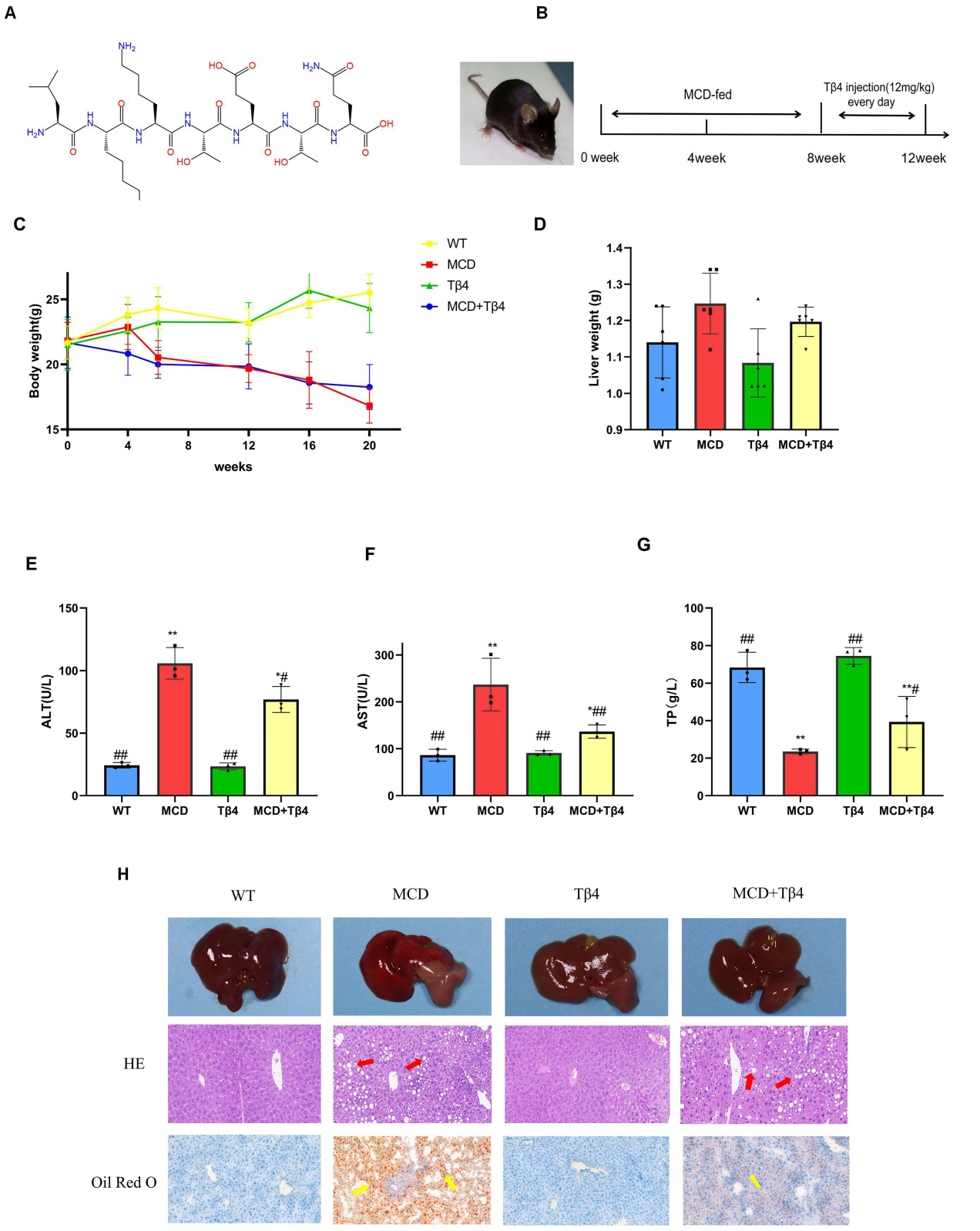

Figure 2 Effects of Tβ4 on biochemical, lipid metabolism and lipid accumulation indices in MCD-induced NAFLD rats. (**A**) Structural formula of the monomer of the active substance of Tβ4. (**B**) Timeline of treatment in Tβ4+MCD group. (**C**) Tβ4 reduces the body weight of NAFLD mice (**D**) Liver weight of mice at execution in different groups. (**E**) Tβ4 reduces serum alanine aminotransferase (ALT) levels in NAFLD mice. (**F**) Tβ4 reduces serum levels of aspartate aminotransferase (AST) in NAFLD mice. (**G**) Tβ4 reduces serum levels of total protein (TP) in NAFLD mice. (**H**) Tβ4 reduces hepatic inflammatory response and lipid accumulation in NAFLD mice. Red and yellow arrows indicate fatty lesions and inflammatory infiltration of the liver. Compared with WT group, *P<0.05 and **P<0.01; compared with MCD group, #P<0.05 and ##P<0.01.

https://doi.org/10.2147/JIR.S492814

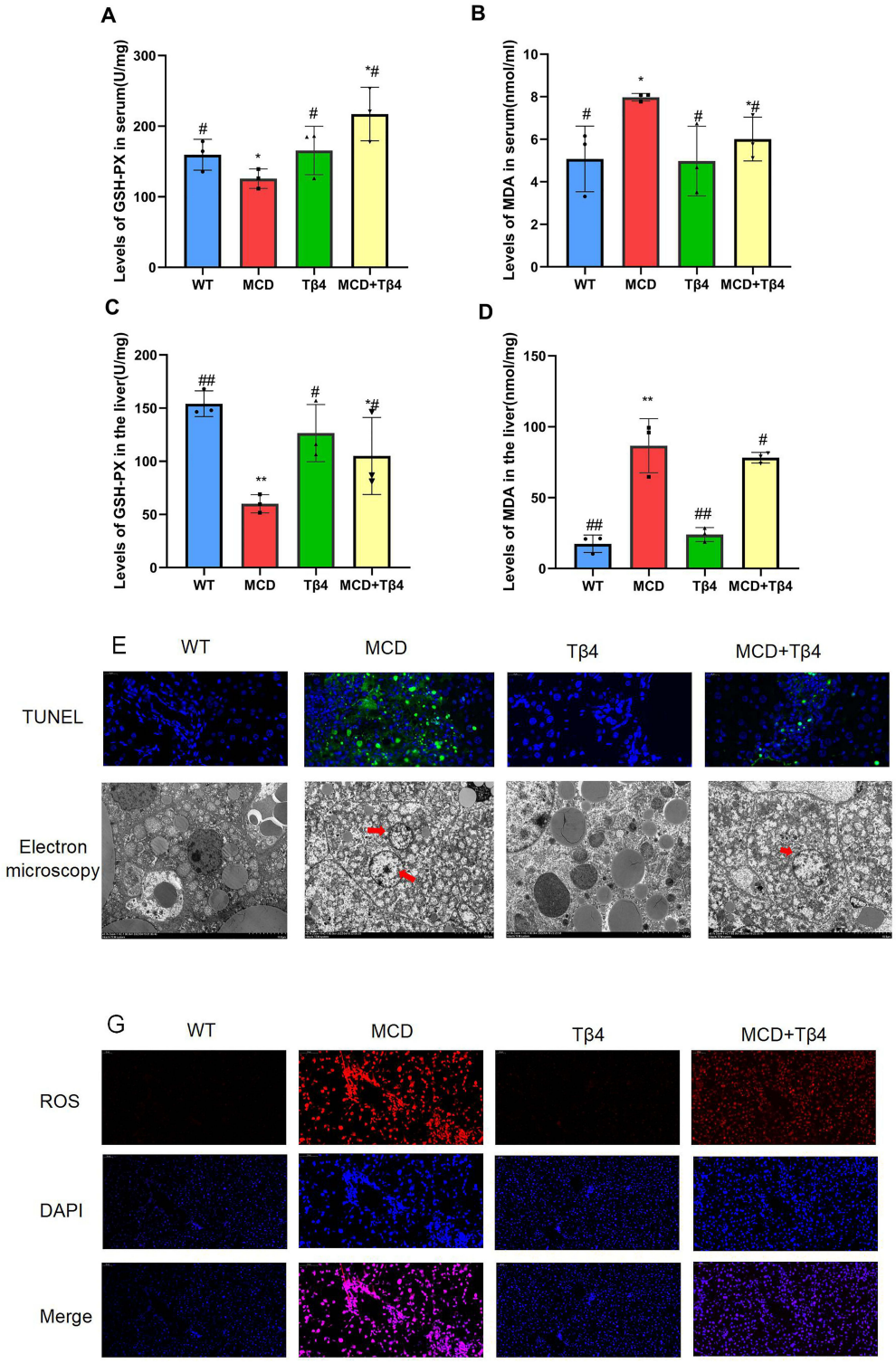

Figure 3 Effect of Tβ4 on antioxidant parameters in MCD-induced NAFLD mice. (**A**) Glutathione peroxidase (GSH-Px) levels in serum of mice in each group. (**B**) Serum levels of malondialdehyde (MDA) in mice in each group. (**C**) Glutathione peroxidase (GSH-Px) levels in the liver of mice in each group. (**D**) Malondialdehyde (MDA) levels in the liver of mice in each group. (**E**) Heavy cell necrosis in the liver of mice in each group. (**F**) Electron microscopy of the livers of mice in each group. (**G**) Tβ4 effectively reduces ROS levels in single-cell suspensions of NAFLD mouse livers (DCFH-DA was used as a probe). All results are the mean of 3 repetitions of the experiment. The normal control group (NC group) was C57 mice fed with regular chow, and the methionine deficient diet model group (MCD group) was mice successfully modelled by methionine choline deficient chow fed for 8 weeks. The Tβ4 group was injected with Tβ4 (12 mg-kg-1-d-1) from week 9 onwards on top of regular chow for a total of 4 weeks. The MCD+Tβ4 group was injected with Tβ4 (12 mg-kg-1-d-1) from week 9 onwards on top of methionine deficient chow fed for a total of 4 weeks. The MCD+Tβ4 group was injected with Tβ4 (12 mg-kg-1-d-1) from week 9 onwards on top of regular chow. Tβ4 (12 mg-kg-1-d-1) injection from week 9 for a total of 4 weeks. The red arrow on the electron microscope shows the damage of organelles. Data are expressed as mean ± S.E.M; *P < 0.05, **P < 0.01, compared with normal control group (WT group). #P < 0.05, ##P < 0.01, compared with the model group (MCD group).

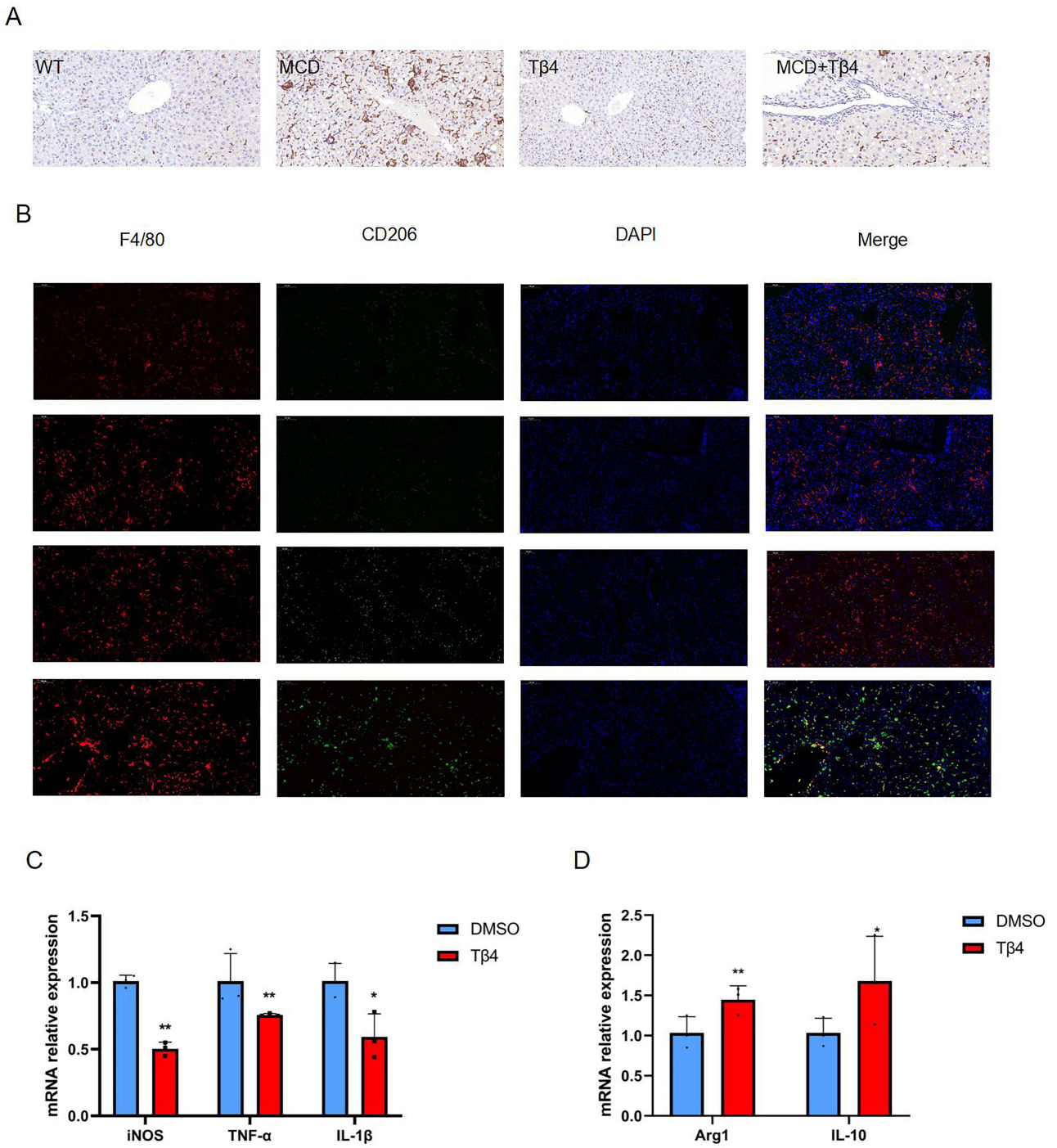

Figure 4 Tβ4 induces macrophage polarisation towards M2 type. (**A**) Liver F4/80 expression in mice of each group. (**B**) Double-stained fluorescence intensity expression of F4/80 and CD206 in the liver of mice in each group. The Tβ4 group was injected with Tβ4 (12 mg-kg-1-d-1) from week 9 onwards for a total of 4 weeks on the basis of regular chow feeding. The MCD+Tβ4 group was injected with Tβ4 (12 mg-kg-1-d-1) from week 9 onwards for a total of 4 weeks on the basis of methionine-deficient chow feeding. Data are expressed as mean ± S.E.M; *P < 0.05, **P < 0.01, compared with normal control group (WT group). #P < 0.05, ##P < 0.01, compared with the model group (MCD group). (**C**) mRNA expression levels of inducible nitric oxide synthase (iNOS), tumour necrosis factor-α (TNF-α) and interleukin 1β (IL-1β) in M1-type macrophages in in vitro experiments. (**D**) mRNA expression levels of arginase 1 (ARG1) and interleukin 10 (IL-10) in M2-type macrophages in the in vitro experiments. The DMSO group was induced by DMSO after isolation of primary mouse hepatic macrophages. The Tβ4 group was induced by Tβ4 after isolation of primary hepatic macrophages, and the induction time was 24 hours for both groups. Data are expressed as mean ± S.E.M; *P < 0.05, **P < 0.01, compared with DMSO group.

Tβ4 (Figure 4B). This part of the experiment, on the basis of the previous part of the experiment, demonstrated that Tβ4 inhibited hepatocyte apoptotic necrosis, regulated hepatic macrophage polarisation and enhanced macrophage anti-inflammatory M2 phenotype. In order to more clearly define the role of Tβ4 in inducing macrophage polarisation, we isolated primary hepatic

https://doi.org/10.2147/JIR.S492814

macrophages from wild-type mice and cultured them under 800 U/mL m-CSF stimulation for 4 days, then added 1000 ng/mL LPS to induce the maturation of primary macrophages, while adding Tβ4 (1000 ng/mL) or DMSO for 24 hours of intervention. Then, mRNA expression of M1 (iNOS, TNF-α and IL-1β) and M2 (ARG1 and IL-10) markers were measured by qPCR. The results showed that the expression of M1 markers was significantly reduced in macrophages treated with Tβ4 compared to control (Figure 4C), whereas the expression of M2 markers was increased (Figure 4D), suggesting that Tβ4 promotes the polarisation of macrophages from the pro-inflammatory M1 subtype to the anti-inflammatory M2 subtype.

Significantly Accelerated NAFLD Progression in Tβ4 Knockdown Mice

The 6-week-old male siRNA Tβ4 mice and WT mice with MCD diet for 3 weeks were induced to model fatty liver in mice. After successful modelling, the mice were switched to normal feed, lentiviral plasmid packed siRNA (1×108 virus titre/dose, 2 times/day) was injected into the tail vein, and liver WB was taken to detect Tβ4 after 4 w to observe the silencing effect. HE staining of liver tissues of mice in both groups showed increased vacuolisation in the liver tissues of siRNA Tβ4 mice (Figure 5A), and more

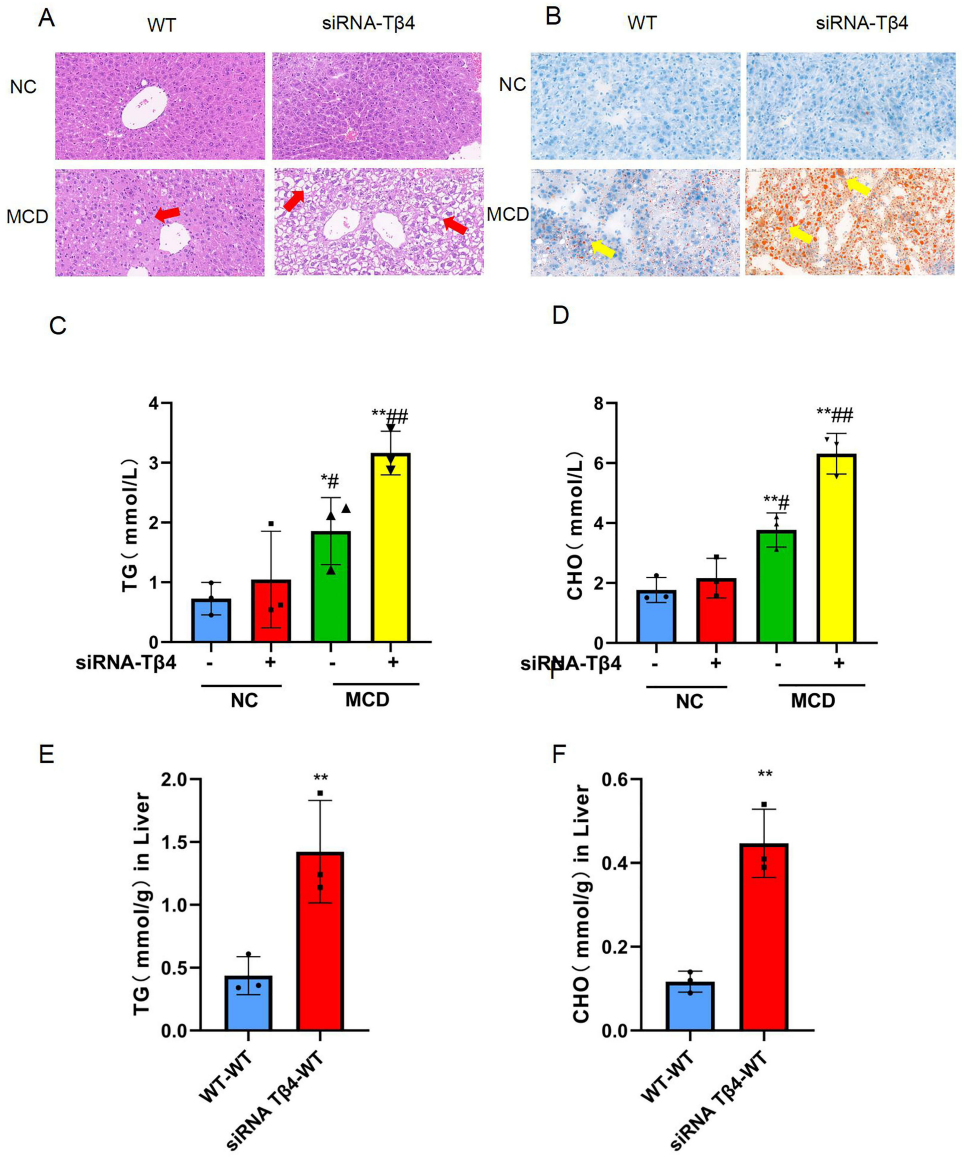

Figure 5 Tβ4 deficiency exacerbates lipid metabolism disorders in mice. (**A**) HE staining of mouse liver in each group. (**B**) Oil-red staining of mouse liver in each group. (**C**) Concentration levels of total triglyceride (TG) in serum of mice in each group. (**D**) Concentration level of total cholesterol (TC) in serum of mice in each group. (**E**) Concentration levels of total triglycerides (TG) in the liver of mice in each group. (**F**) Concentration levels of total cholesterol (TC) in the livers of mice in each group. Data are expressed as mean ± S.E.M; Red and yellow arrows indicate fatty lesions and inflammatory infiltration of the liver. *P < 0.05, **P < 0.01, compared with NC-WT group. #P < 0.05, ##P < 0.01, compared with NC-siRNA.

pronounced accumulation of oil red O (OilredO) (Figure 5B), and a tendency to inflammatory reactions and balloon-like changes in hepatocytes even when regular feed feeding was applied. Serum TG and total cholesterol (CHO) assays in mice and liver tissue homogenates revealed significant lipid metabolism disorders in siRNA Tβ4 mice compared with WT mice (Figure 5C–F).

Macrophage Depletion Impairs the Therapeutic Efficacy of Tβ4 for NAFLD Treatment

As known from Figures 4 and 5, excessive oxidative stress within NAFLD induces macrophages to polarise towards pro-inflammatory phenotype, releasing more pro-inflammatory cytokines, which in turn exacerbates steatosis; whereas, Tβ4 plays an important role in regulating macrophage phenotypic polarisation, and knockdown of Tβ4 promotes hepatic macrophages to polarise towards the pro-inflammatory M1 type. To further illustrate that the inhibitory effect of Tβ4 on fatty liver is mediated through macrophages. First, we constructed a mouse model of macrophage depletion by intraperitoneal injection of liposome polyphosphate, in which F4/80 serves as a highly specific macrophage marker. Injection of sodium clodronate liposomes can eliminate mouse liver macrophages. As shown in Figure 6A, sodium clodronate consumption resulted in mild hepatic steatosis, reduced lobular inflammatory infiltration, and relatively less ballooning. There were also differences in glucose tolerance and insulin resistance between the two groups. Mice with clodronate depletion that were also treated with t-β4 showed the most significant metabolic improvement (Figure 6B–C). It is worth noting that serum aminotransferase (Figure 6D–E) and lipid levels (Figure 6F–G) were most significantly improved in the Tβ4 treatment group alone, suggesting that the improvement of Tβ4 on fatty liver may be mediated by regulating the production of macrophages. If macrophages are depleted and the inflammatory response intensifies (Figure 6H–I), the therapeutic effect of Tβ4 appeared to be attenuated.

Proteomic Analysis Reveals That Tβ4 Treatment Effect Correlates with STAT1 Signalling Pathway

To further analyse the Tβ4-associated signalling pathways, we performed liver hepatic proteomic analysis in MCD and MCD +Tβ4 mice. Liver samples were analysed using LC-MS, raw data were merged and searched using MaxQuant 1.5.3.17 software for identification and quantitative analysis. The use of Cluster 3.0 (http://bonsai.hgc.jp/~mdehoon/software/cluster/software.htm) and Java Treeview software (http://jtreeview.sourceforge.net) were used to perform stratification clustering analysis. For hierarchical clustering, the Euclidean distance algorithm was chosen as the similarity measure and the average linkage clustering algorithm (which uses the centroids of the observations when clustering) was chosen for clustering, which was presented as a heatmap (Figure 7A). And then the studied proteins were compared with the online Kyoto Encyclopedia of Genes and Genomes (KEGG) database (http://geneontology.org/) to retrieve their KEGG orthologous identifications and subsequently mapped to pathways in KEGG (Figure 7B). The proteomic analysis showed that the therapeutic effect after Tβ4 may be related to the STAT1 signalling pathway. To further clarify the proteomic results, Western blotting was applied to validate the results in each group of mice. It is suggested that Tβ4 may reduce recruitment of inflammatory cytokines by increasing the expression of SOCS1 and SOCS3 in the cytokine signaling suppressor (SOCSs) family, thereby negatively regulating the expression of STAT1 (Figure 7C–I).

Tβ4 Attenuates Hepatocyte Injury by Affecting Macrophage Polarisation Responses

The schematic of cell co-culture model is detailed in Figure 8A. LO2 cell supernatants were taken for AST and ALT levels. Compared with the model group (LPS-stimulated group), all treatment groups of Tβ4 reduced the CCl4 damage effect ($P < 0.05$). The low concentration dose group (10ng/mL) had a tendency to decrease though, and the improvement was mild compared with the high concentration dose group (1000ng/mL) (Figure 8B–C). Therefore, the therapeutic effect of Tβ4 is proportional to the therapeutic concentration. As can be seen from Figure 8D, the cell apposition ability of the model group was significantly weakened, and the degree of cell damage was obvious. The cell damage effect of the Tβ4 treatment group was significantly weakened with the increase of the drug concentration. The proportion of wall-adherent cells increased and the proportion of necrotic cells decreased. C2 area (PI+/AnnexinV+) indicated late apoptosis and C4 area (PI-/AnnexinV+) indicated early apoptosis. The assay results showed (Figure 8E) that flow cytometry detected a large amount of apoptosis in the Model group (Figure 8E-b), and the overall apoptosis rate was reduced in

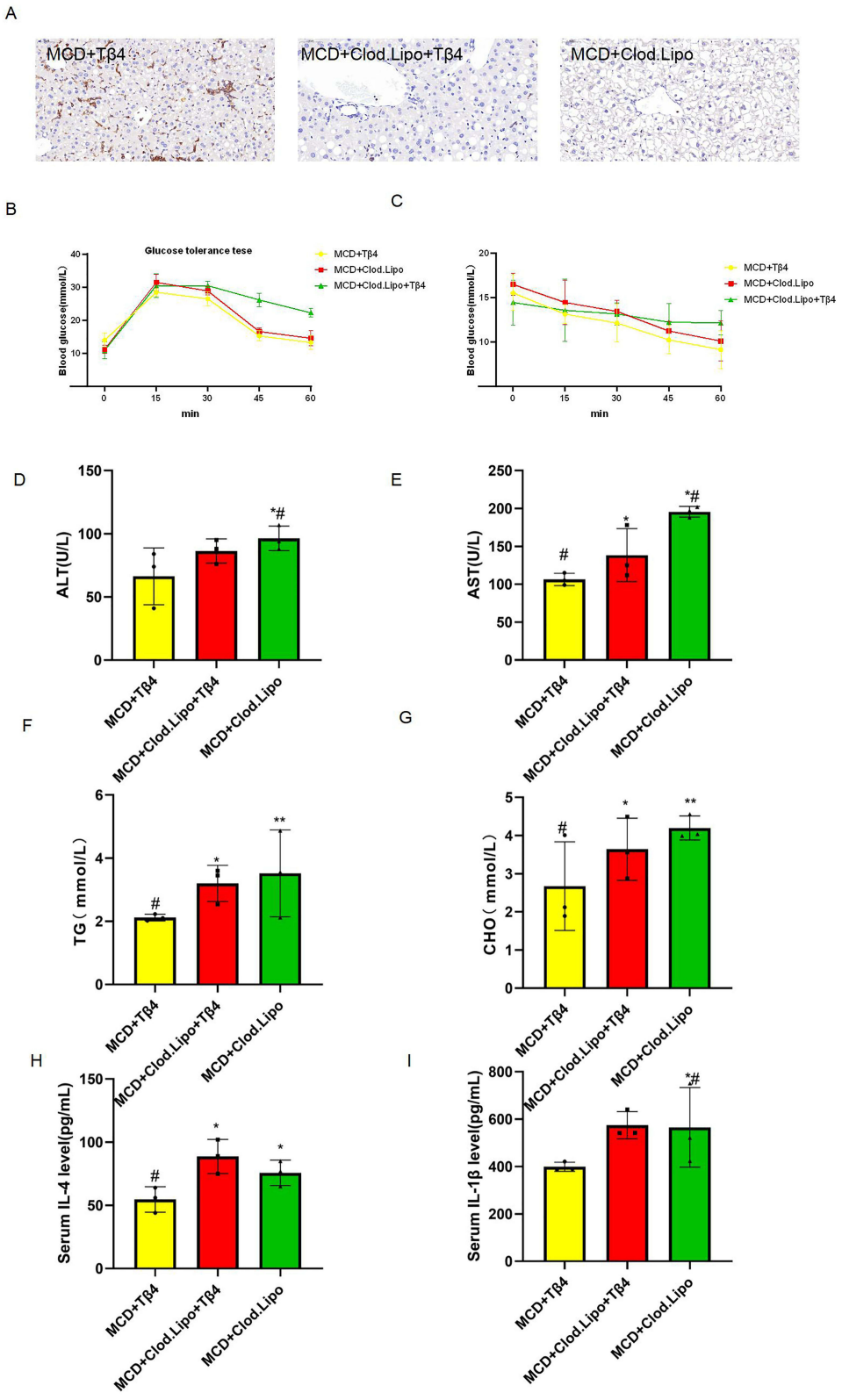

Figure 6 Tβ4 modulates macrophage polarisation to ameliorate hepatic inflammation and lipid metabolism disorders in mice. (**A**) Immunohistochemistry of mouse liver F4/80 in each group. (**B**) Glucose tolerance test in mice of each group. (**C**) Insulin resistance assay in each group of mice. (**D**) Concentration level of ALT in serum of each group of mice. (**E**) Concentration levels of AST in serum of each group of mice. (**F**) Concentration levels of total triglycerides (TG) in serum of mice in each group. (**G**) Concentration levels of total triglycerides (TG) in serum of mice in each group. (**H**) Concentration levels of interleukin 4 in serum of mice in each group. (**I**) Concentration levels of interleukin 1β in serum of mice in each group. Data are expressed as mean ± S.E.M; *P < 0.05, **P < 0.01, compared with MCD+Tβ4 group. #P < 0.05, ##P < 0.01, compared with MCD+Clod.Lipo+Tβ4 group.

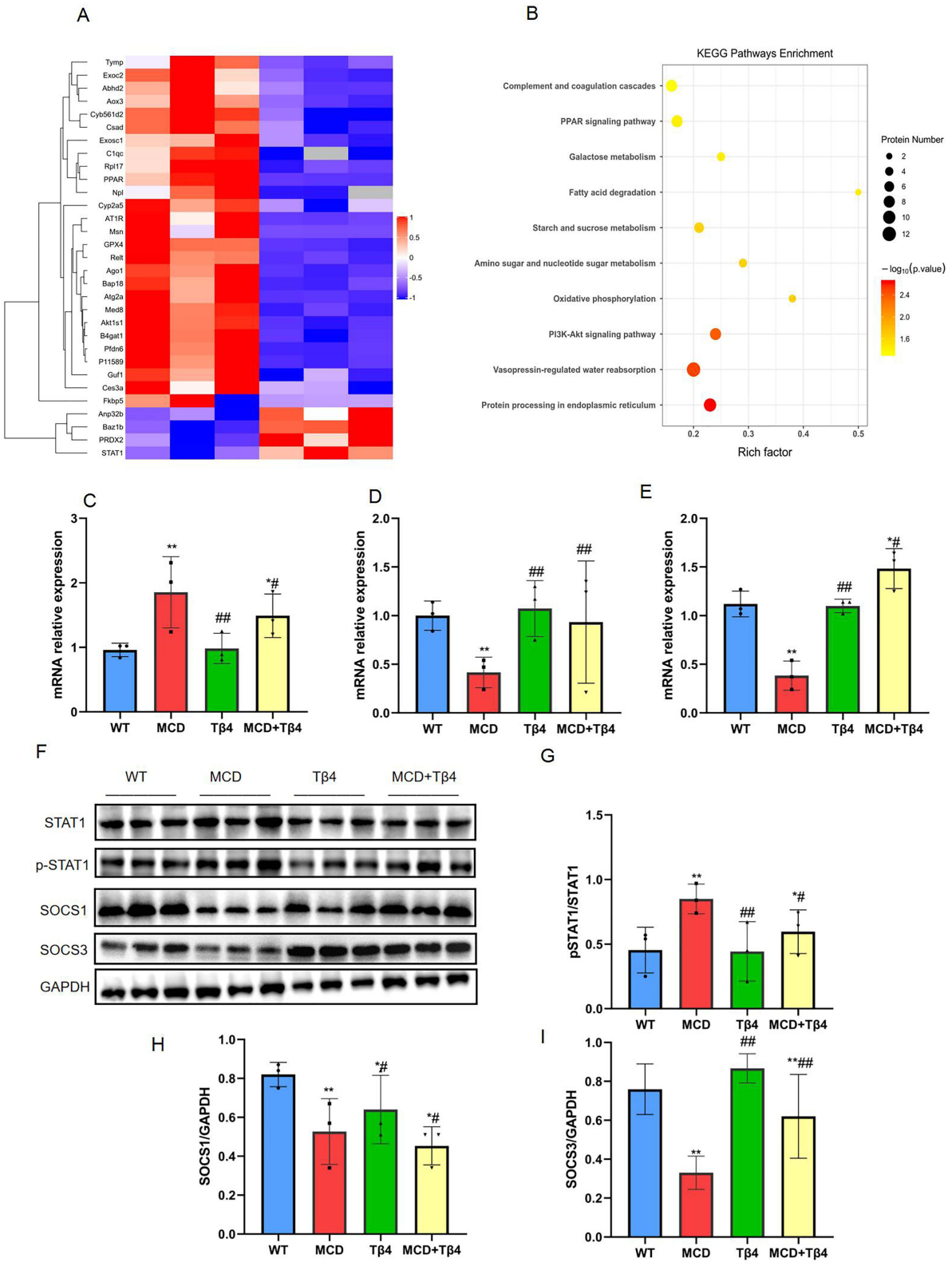

Figure 7 Tβ4 improves NAFLD by regulating the STAT1/SOCS1 signaling pathway. (**A**) Protein cluster heat map of MCD and MCD+Tβ4 mice (**B**) Enrichment map of KEGG-related signaling pathway of Tβ4 treated NAFLD mice (**C**) liver STAT1 mRNA level of mice in each group (**D**) liver SOCS1 mRNA level of mice in each group (**E**) liver SOCS3 mRNA level of mice in each group (**F**) Liver STAT1 signaling pathway protein expression of mice in each group (**G**) liver p-STAT1 protein level of mice in each group (**H**) liver SOCS1 protein level of mice in each group (**I**) liver SOCS3 protein level of mice in each group. Data are expressed as mean ±S.E.M. *P < 0.05, **P < 0.01, compared with WT group. $^{\#}$P < 0.05, $^{\#\#}$P < 0.01, compared with MCD group.

https://doi.org/10.2147/JIR.S492814

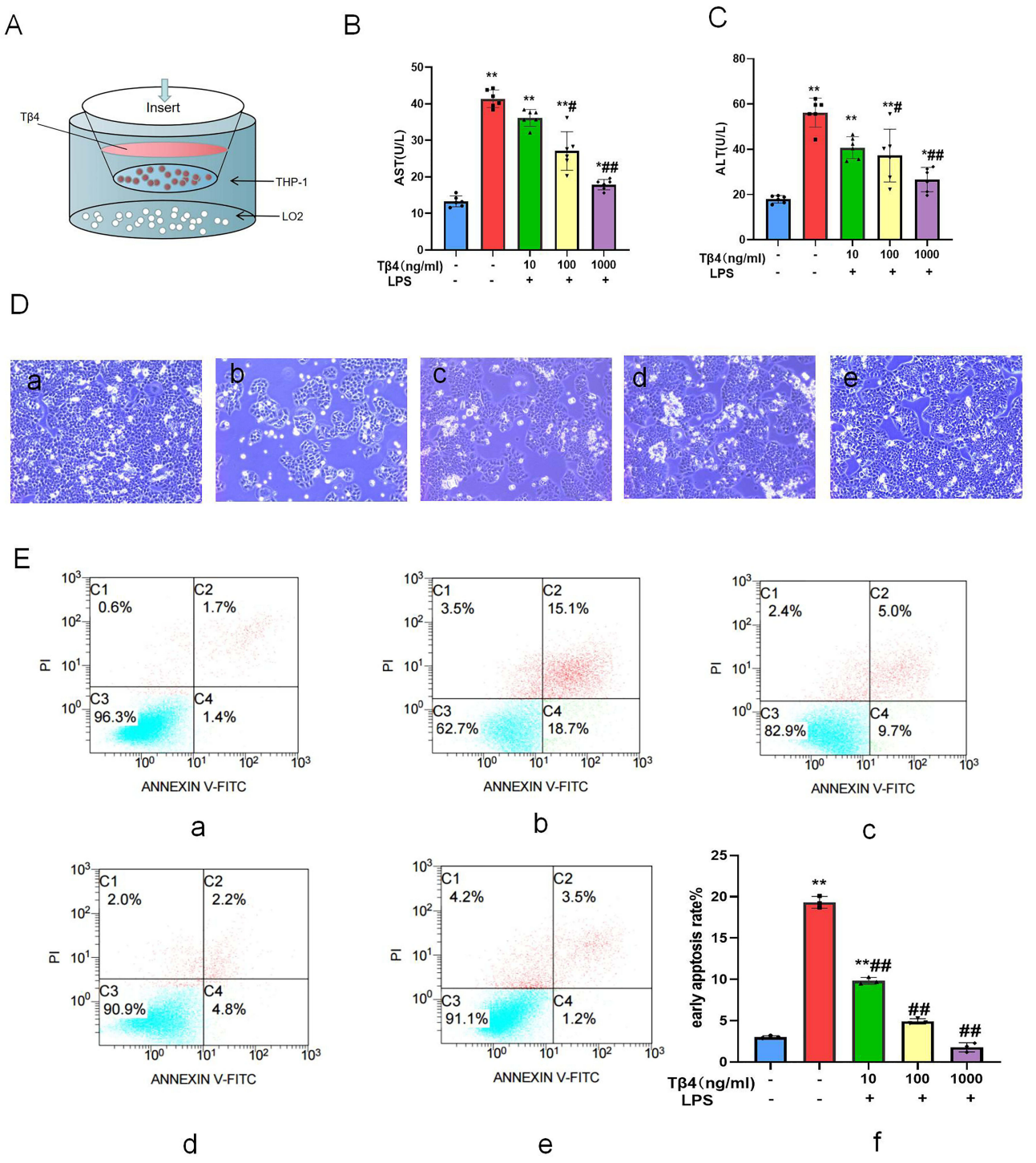

Figure 8 Tβ4 ameliorates hepatocyte injury after cell co-culture.(**A**) Schematic diagram of cell co-culture pattern (**B**) Tβ4 enhanced fine blog M2 polarization of macrophages and decreased serum alanine aminotransferase (ALT) levels in the supernatant of LO2 cells. (**C**) Tβ4 enhancement of M2-type polarization in macrophages decreased serum aspartate aminotransferase (AST) levels in the supernatant of LO2 cells. (**D**) Apoptosis and necrosis of cells in each group under optical microscope. D-A was the group without Tβ4 and LPS.D-b was LPS stimulated group, c-e was LPS stimulated Tβ4 intervention concentration of 10,100,1000ng/mL.(**E**) Detection of apoptosis of LO2 cells by Tβ4 in AnnexinV/PI co-culture system. Cell apoptosis was late in C2 quadrant and early in C4 quadrant. All data were repeated three times, and the a-e group was the same as that of (**D**). The assay results showed (**E**) that flow cytometry detected a large amount of apoptosis in the Model group (**E**-b), and the overall apoptosis rate was reduced in both Tβ4-treated groups (**E** c-e) compared with the Model group, suggesting that the effect of Tβ4 in ameliorating LO2 injury involves the whole process of apoptosis in both the early and late stages of the cell death. All data were replicated three times and expressed as mean ± S.E.M *p<0.05 and **p<0.01 compared with Tβ4(-)/LPS(-) group; $^{\#}$p<0.05 and $^{\#\#}$p<0.01 compared with Tβ4(-)/LPS(+) group.

both Tβ4-treated groups (Figure 8E c-e) compared with the Model group, suggesting that the effect of Tβ4 in ameliorating LO2 injury involves the whole process of apoptosis in both the early and late stages of the cell death.

Tβ4 Attenuates ROS Accumulation by LO2 and Reduces STAT1 Signalling Pathway Expression

ROS levels were shown using the DCFH-DA probe (Figure 9A). Serum ROS levels were significantly higher in the LPS group compared to the NC group. Compared with the Model group, ROS levels were significantly lower in the Tβ4-treated group. This indicated that Tβ4 could alleviate the cumulative damage of ROS to LO2 cells.

The previous results revealed that STAT1 and its downstream pathway proteins were significantly reduced in MCD-bred mice treated with Tβ4 (Figure 9). To investigate whether Tβ4 attenuated the pro-inflammatory response of macrophages through the STAT1 pathway. Fluorescent expression of p-STAT1 expression was significantly increased in the model group (Figure 9B), suggesting that p-STAT1 was phosphorylated to an increased extent in oleic acid-modelled hepatocytes. Compared with the model, p-STAT1 expression was significantly attenuated in the treatment group. The fluorescence intensity was negatively correlated with the Tβ4 dose.

Discussion

NAFLD is a clinicopathological syndrome characterised by diffuse hepatocellular vesicular steatosis due to factors other than alcohol and other well-defined liver injury.[13] It is a clinicopathological syndrome characterised by diffuse hepatocellular steatosis and includes non-alcoholic simple fatty liver disease, non-alcoholic steatohepatitis (and its associated cirrhosis and hepatocellular carcinoma.[14] Among them, NASH is the most serious type, which refers to an inflammatory reaction of the liver parenchyma characterised by hepatocellular steatosis, diffuse hepatic lobular mild inflammation and or collagen deposition around the central hepatic vein and hepatic sinusoids, with the main pathological features of mixed inflammatory cell infiltration, balloon-like degeneration, and microsomal formation in the hepatic follicular zone III and the portal ductal zone.[15] With the improvement of people's living standards, changes in dietary structure and behaviour, the incidence of the disease has shown an increasing trend year by year, and it is an important cause of cryptogenic cirrhosis, which is a serious danger to people's health.[16]

In the present study, we found that the level of serum Tβ4 was significantly lower in patients compared to healthy controls. The level of serum Tβ4 in patients with NAFLD may better reflect the function of the liver.[17] The cause of poor liver function in patients is closely related to its pathogenesis When it occurs, fatty acid overload occurs and mitochondrial fatty acid oxidation is impaired, unoxidised fatty acids are continuously esterified to generate triacylglycerol, which is deposited in the hepatocytes, leading to hepatocellular steatosis. Abnormal accumulation of liver fat and steatosis will lead to abnormal endoplasmic reticulum and mitochondrial function, further aggravating oxidative stress and lipid peroxidation, causing a vicious circle, and severely impairing the hepatocyte function of patients.[18] In this study, the serum levels of patients were detected by the method, and it was found that the serum concentration of NAFLD patients was lower than that of healthy people, and it was significantly higher after effective treatment. Meanwhile, immunofluorescence staining of paracancerous tissues from patients with non-fat-associated HCC and those with fat-associated HCC revealed that Tβ4 expression was significantly lower in patients with fat-associated HCC. In order to further illustrate the association between Tβ4 and NAFLD, the GSE dataset and the corresponding platform file were downloaded to obtain GPL13534 expression profile data, and the platform file was used to complete the ID conversion, and after that, using the limma package, data correction was carried out for the 2 expression profiles data and the log value was taken, respectively, and finally, a box-and-line diagram was used to visualise the Tβ4 expression, and the analysis concluded that with the severity of fatty liver progressed, the expression of Tβ4 was gradually decreasing.

Our study shows that Tβ4 is protective against MCD-induced NAFLD and inhibits hepatocellular steatosis by modulating macrophage polarization.[19] First, Tβ4 inhibited lipid accumulation in the liver.[20] Secondly, Tβ4 attenuated MCD-induced hepatocyte apoptosis and mitochondrial damage, inhibited macrophage-associated inflammatory responses in liver tissue, and regulated macrophage polarisation. ROS-induced oxidative stress caused cellular damage, triggering

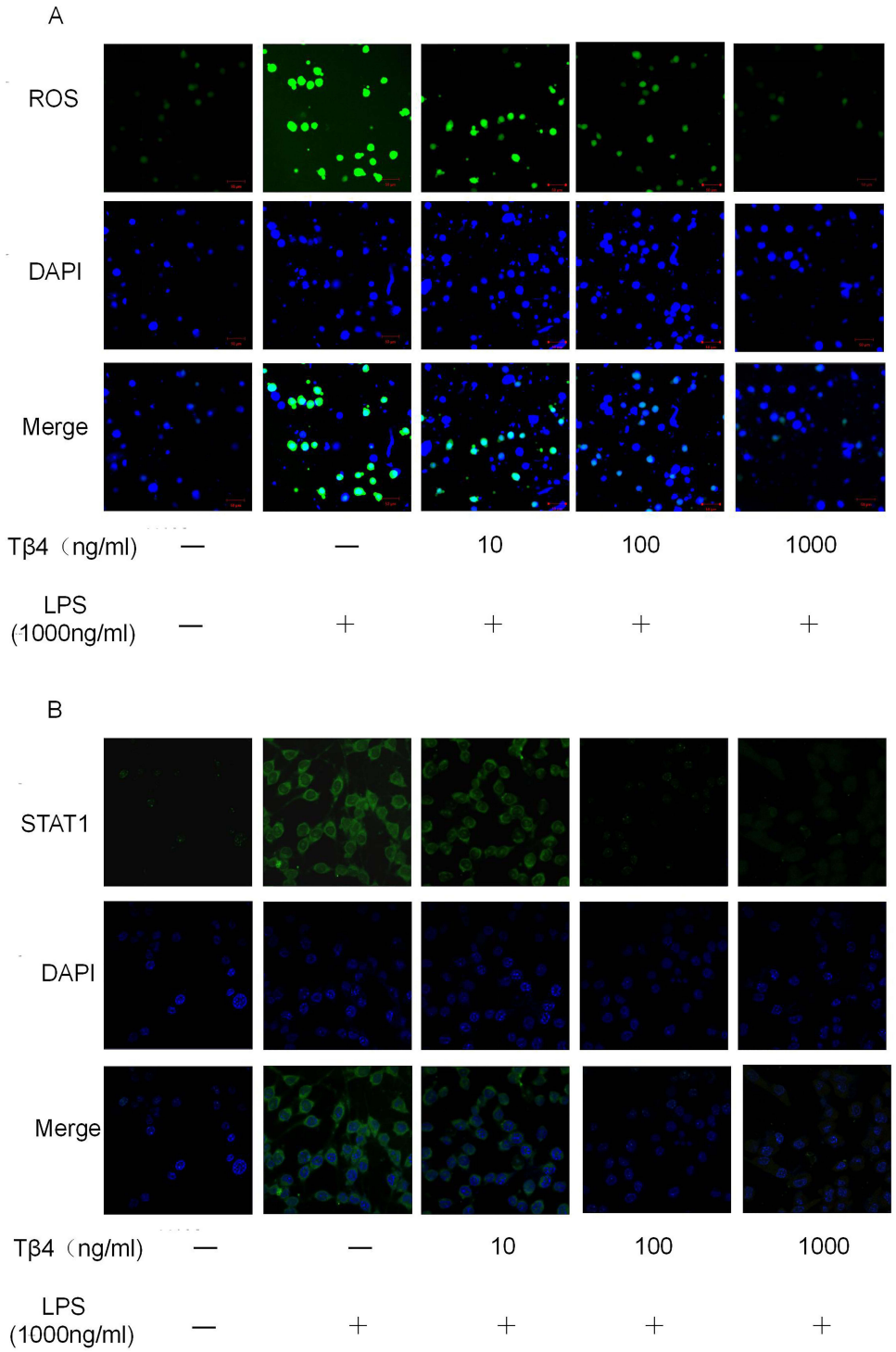

Figure 9 Tβ4 inhibits STAT phosphorylation in hepatocytes after cell co-culture. (**A**) Tβ4 effectively reduced ROS levels in LO2 cells in cell co-culture experiments. (**B**) Immunofluorescence localisation assay (n=3) was used to observe STAT phosphorylation levels in LO2 cells. Green fluorescence represents p-STAT expression, and fluorescence intensity is proportional to protein expression. Blue: cell nuclei stained with DAPI; Merge: first two images overlapped; Scale bar: 100 μm.

the onset of inflammation and hepatic fibrosis formation in NAFLD.[21] Clinical trials and animal studies have confirmed that ROS inhibitors or antioxidants have significant ameliorating effects in NAFLD, clarifying the key role of ROS in the inflammatory process of NASH.[22] Although oxygen-containing free radical molecules can cause direct cellular damage, excessive ROS accumulation is still effective in initiating the oxygen-sensitive nuclear transcription factor STAT1,[23]

which promotes inflammatory cytokines such as IL-1β and TNF-α. In the present study, aberrant lipid accumulation was found in the livers of siRNA-Tβ4 mice, with significantly elevated levels of triglyceride and total cholesterol in serum and liver, and disorders of abnormal lipid metabolism were observed.[24]

And the dynamic balance of M1 /M2 macrophages may be critical for Tβ4 to ameliorate the progression of NAFLD [This study explored this balance in a mouse model of fatty liver.

To more further illustrate the direct effect of Tβ4 on macrophage polarisation, we cultured wild-type mouse primary macrophages in an in vitro environment and directly intervened with Tβ4 and a control solvent (DMSO). According to qPCR assay, the mRNA levels of these pro-inflammatory macrophage (M1) markers, such as TNF-α, IL-1β, and iNOS, were low in Kupffer cells exposed to Tβ4, whereas the anti-inflammatory macrophage (M2) markers (ARG1, IL-10) were relatively low. This suggests that Tβ4 can regulate macrophage polarisation towards the anti-inflammatory type, thus exerting a protective effect against macrophage-mediated inflammatory responses in NAFLD mice, which can also be used to explain the efficacy of Tβ4 in NAFLD mice. At the same time, the therapeutic effect of Tβ4 was attenuated by depletion of hepatic macrophages by chlorophosphate. It is suggested that Tβ4 may have been used to enhance macrophage M2 polarisation and thus slow down the NAFLD process.[25]

To more further illustrate the direct effect of Tβ4 on macrophage polarisation, we cultured wild-type mouse primary macrophages in an in vitro environment and directly intervened with Tβ4 and a control solvent (DMSO). According to qPCR assay, the mRNA levels of these pro-inflammatory macrophage (M1) markers, such as TNF-α, IL-1β, and iNOS, were low in Kupffer cells exposed to Tβ4, whereas the anti-inflammatory macrophage (M2) markers (ARG1, IL-10) were relatively low. This suggests that Tβ4 can regulate macrophage polarisation towards the anti-inflammatory type, thus exerting a protective effect against macrophage-mediated inflammatory responses in NAFLD mice, which can also be used to explain the efficacy of Tβ4 in NAFLD mice.[26] At the same time, the therapeutic effect of Tβ4 was attenuated by depletion of hepatic macrophages by chlorophosphate.[27] It is suggested that Tβ4 may have been used to enhance macrophage M2 polarisation and thus slow down the NAFLD process.[28]

Previous studies have shown that Tβ4 can inhibit the NF-κB signaling pathway, thereby reversing the phenotypic differentiation of glial cells and improving cognitive impairment.[29] However, previous articles of our research group have shown that Tβ4 can reduce the degree of liver fibrosis by slowing down the release of factors related to NF-κB signaling pathway.[30,31] This study also showed that Tβ4 enhanced intracellular antioxidant activity by up-regulating SOCS1 and SOCS3 expression, thereby alleviating liver LO2 cell damage. Meanwhile, studies have shown that over-expression of SOCS1 and SOCS3 can inhibit the activation of STAT pathway inflammatory response. Whether Tβ4 can attenuate NAFLD by modulating other signaling pathways is unclear.[32] In follow-up experiments, the use of more specific small molecule inhibitors or conditional knockout mice will help further verify the detailed molecular mechanisms by which Tβ4 exerts its protective effect.

Conclusion

This study confirmed that Tβ4 showed negative correlation in NAFLD disease progression. And Tβ4 can regulate macrophage polarisation and produce anti-inflammatory effects, further reducing hepatocyte steatosis and cellular damage, providing a new and novel direction for clinical prevention and treatment of NAFLD.

Data Sharing Statement

The datasets used and/or analyzed during the current study are available from the corresponding author on reasonable request.

Ethics Approval and Consent to Participate

All the animal experiments presented in this research were approved and supervised by the Animal Care Welfare Committee of Guizhou Medical University, China, No.200962, and all operations were performed in accordance with the Guide for the Care and Use of Laboratory Animals of China.

Author Contributions

All authors made a significant contribution to the work reported, whether that is in the conception, study design, execution, acquisition of data, analysis and interpretation, or in all these areas; took part in drafting, revising or critically reviewing the article; gave final approval of the version to be published; have agreed on the journal to which the article has been submitted; and agree to be accountable for all aspects of the work.

Funding

This study was supported by the National Natural Science Foundation (Grant No. 82360134); the Science and Technology Fund project of Guizhou Provincial Health Commission (Grant no. [2022]180); the Science and Technology Fund project of Guizhou Provincial Health Commission (Grant no.[2024]115); the Doctor Start-up Fund of Affiliated Hospital of Guizhou Medical University (Grant no. [2023]11); the Affiliated Hospital of Guizhou Medical University National Natural Science Foundation cultivation program (Grant no.[2023]36) and Guizhou Provincial Basic Research Program(Natural Science) (Approval No.QKHJC-zk2025449).

Disclosure

The authors declare no competing interests in this work.

References

1. Friedman SL, Neuschwander-Tetri BA, Rinella M, Sanyal AJ. Mechanisms of NAFLD development and therapeutic strategies. *Nat Med*. 2018;24(7):908–922. doi:10.1038/s41591-018-0104-9
2. Pouwels S, Sakran N, Graham Y, et al. Non-alcoholic fatty liver disease (NAFLD): a review of pathophysiology, clinical management and effects of weight loss. *BMC Endocr Disord*. 2022;22(1):63. doi:10.1186/s12902-022-00980-1
3. Tilg H, Adolph TE, Moschen AR. Multiple parallel hits hypothesis in nonalcoholic fatty liver disease: revisited after a decade. *Hepatology*. 2021;73(2):833–842. doi:10.1002/hep.31518
4. Barreby E, Chen P, Aouadi M. Macrophage functional diversity in NAFLD - more than inflammation. *Nat Rev Endocrinol*. 2022;18(8):461–472. doi:10.1038/s41574-022-00675-6
5. Gao H, Jin Z, Bandyopadhyay G, et al. MiR-690 treatment causes decreased fibrosis and steatosis and restores specific Kupffer cell functions in NASH. *Cell Metab*. 2022;34(7):978–990. doi:10.1016/j.cmet.2022.05.008
6. Fan N, Zhang X, Zhao W, et al. Covalent inhibition of pyruvate kinase M2 reprograms metabolic and inflammatory pathways in hepatic macrophages against non-alcoholic fatty liver disease. *Int J Biol Sci*. 2022;18(14):5260–5275. doi:10.7150/ijbs.73890
7. Handa P, Thomas S, Morgan-Stevenson V, et al. Iron alters macrophage polarization status and leads to steatohepatitis and fibrogenesis. *J Leukoc Biol*. 2019;105(5):1015–1026. doi:10.1002/JLB.3A0318-108R
8. Dong B, Zhou Y, Wang W, et al. Vitamin D receptor activation in liver macrophages ameliorates hepatic inflammation, steatosis, and insulin resistance in mice. *Hepatology*. 2020;71(5):1559–1574. doi:10.1002/hep.30937
9. Bijnen M, Josefs T, Cuijpers I, et al. Adipose tissue macrophages induce hepatic neutrophil recruitment and macrophage accumulation in mice. *Gut*. 2018;67(7):1317–1327. doi:10.1136/gutjnl-2016-313654
10. Xing Y, Ye Y, Zuo H, Li Y. Progress on the function and application of thymosin β4. *Front Endocrinol*. 2021;12:767785. doi:10.3389/fendo.2021.767785
11. Belsky JB, Rivers EP, Filbin MR, Lee PJ, Morris DC. Thymosin beta 4 regulation of actin in sepsis. *Expert Opin Biol Ther*. 2018;18(sup1):193–-197. doi:10.1080/14712598.2018.1448381
12. Zhu Z, Zhang Y, Huang X, et al. Thymosin beta 4 alleviates non-alcoholic fatty liver by inhibiting ferroptosis via up-regulation of GPX4. *Eur J Pharmacol*. 2021;908:174351. doi:10.1016/j.ejphar.2021.174351
13. Rong L, Zou J, Ran W, et al. Advancements in the treatment of non-alcoholic fatty liver disease (NAFLD). *Front Endocrinol*. 2023;13:1087260. doi:10.3389/fendo.2022.1087260
14. Eslam M, Sanyal AJ, George J. International consensus panel. MAFLD: a consensus-driven proposed nomenclature for metabolic associated fatty liver disease. *Gastroenterology*. 2020;158(7):1999–2014.e1. doi:10.1053/j.gastro.2019.11.312
15. Paternostro R, Trauner M. Current treatment of non-alcoholic fatty liver disease. *J Intern Med*. 2022;292(2):190–204. doi:10.1111/joim.13531
16. Harrison SA, Allen AM, Dubourg J, Noureddin M, Alkhouri N. Challenges and opportunities in NASH drug development. *Nat Med*. 2023;29(3):562–573. doi:10.1038/s41591-023-02242-6
17. Xu H, Zhao Q, Song N, et al. AdipoR1/AdipoR2 dual agonist recovers nonalcoholic steatohepatitis and related fibrosis via endoplasmic reticulum-mitochondria axis. *Nat Commun*. 2020;11(1):5807. doi:10.1038/s41467-020-19668-y
18. Flessa CM, Kyrou I, Nasiri-Ansari N, Kaltsas G, Kassi E, Randeva HS. Endoplasmic reticulum stress in nonalcoholic (metabolic associated) fatty liver disease (NAFLD/MAFLD). *J Cell Biochem*. 2022;123(10):1585–1606. doi:10.1002/jcb.30247
19. Vonderlin J, Chavakis T, Sieweke M, Tacke F. The multifaceted roles of macrophages in NAFLD pathogenesis. *Cell Mol Gastroenterol Hepatol*. 2023;15(6):1311–1324. doi:10.1016/j.jcmgh.2023.03.002
20. Xiao Z, Liu M, Yang F, et al. Programmed cell death and lipid metabolism of macrophages in NAFLD. *Front Immunol*. 2023;14:1118449. doi:10.3389/fimmu.2023.1118449

21. Ma C, Kesarwala AH, Eggert T, et al. NAFLD causes selective CD4(+) T lymphocyte loss and promotes hepatocarcinogenesis. *Nature*. 2016;531 (7593):253–257. doi:10.1038/nature16969
22. Chen Z, Tian R, She Z, Cai J, Li H. Role of oxidative stress in the pathogenesis of nonalcoholic fatty liver disease. *Free Radic Biol Med*. 2020;152:116–141. doi:10.1016/j.freeradbiomed.2020.02.025
23. Xu Z, Xi F, Deng X, et al. Osteopontin promotes macrophage M1 polarization by activation of the JAK1/STAT1/HMGB1 signaling pathway in nonalcoholic fatty liver disease. *J Clin Transl Hepatol*. 2023;11(2):273–283. doi:10.14218/JCTH.2021.00474
24. Dong Y, Yu C, Ma N, et al. MicroRNA-379-5p regulates free cholesterol accumulation and relieves diet induced-liver damage in db/db mice via STAT1/HMGCS1 axis. *Mol Biomed*. 2022;3(1):25. doi:10.1186/s43556-022-00089-w
25. Loureiro D, Tout I, Narguet S, et al. Mitochondrial stress in advanced fibrosis and cirrhosis associated with chronic hepatitis B, chronic hepatitis C, or nonalcoholic steatohepatitis. *Hepatology*. 2023;77(4):1348–1365. doi:10.1002/hep.32731
26. Mosca A, Crudele A, Smeriglio A, et al. Antioxidant activity of hydroxytyrosol and vitamin E reduces systemic inflammation in children with paediatric NAFLD. *Dig Liver Dis*. 2021;53(9):1154–1158. doi:10.1016/j.dld.2020.09.021
27. Ke X, Zhang R, Li P, et al. Hydrochloride Berberine ameliorates alcohol-induced liver injury by regulating inflammation and lipid metabolism. *Biochem Biophys Res Commun*. 2022;610:49–55. doi:10.1016/j.bbrc.2022.04.009
28. Luo Y, Chen Q, Zou J, Fan J, Li Y, Luo Z. Chronic intermittent hypoxia exposure alternative to exercise alleviates high-fat-diet-induced obesity and fatty liver. *Int J Mol Sci*. 2022;23(9):5209. doi:10.3390/ijms23095209
29. Wang M, Feng LR, Li ZL, et al. Thymosin β4 reverses phenotypic polarization of glial cells and cognitive impairment via negative regulation of NF-κB signaling axis in APP/PS1 mice. *J Neuroinflamm*. 2021;18(1):146. doi:10.1186/s12974-021-02166-3
30. Wang Z, Zhang Y, Wang Y, Mou Q, Ren T, Zhu L. Mechanism of thymosin β4 in ameliorating liver fibrosis via the MAPK/NF-κB pathway. *J Biochem Mol Toxicol*. 2023;37(7):e23338. doi:10.1002/jbt.23338
31. Zhu ZX, Zhu LL, Cheng Z, et al. Cellular mechanism of Tβ4 intervention in liver fibrosis by regulating NF-κB signaling pathway. *Eur Rev Med Pharmacol Sci*. 2019;23(3):1279–1290. doi:10.26355/eurrev_201902_17023
32. Bai J, Chen S. LncRNA CASC9 enhances the stability of SOCS-1 by combining with FUS to alleviate sepsis-induced liver injury. *Cytokine*. 2023;171:156346. doi:10.1016/j.cyto.2023.156346